Optical Spectroscopy during Growth of PTCDA-C_{60} Complex Thin Films

Sunggook Park,*,† Dmitri A. Tenne,†,‡ Georgeta Salvan,† Thorsten U. Kampen,† and Dietrich R. T. Zahn†

Halbleiterphysik, TU Chemnitz, D-09107 Chemnitz, Germany, and Institute of Semiconductor Physics, 630090 Novosibirsk, Russia

Received: May 21, 2001

Combined Raman and photoluminescence (PL) measurements were performed in situ and online during the formation of a PTCDA-C_{60} charge transfer (CT) complex film using organic molecular beam deposition. It is found that two different processes compete during growth, namely the formation of PTCDA-C_{60} CT complexes and the photopolymerization between C_{60} molecules. The CT complexes, formed instantaneously upon the co-deposition of two molecules, decompose as the C_{60} molecules forming the CT complexes undergo the photopolymerization with excess C_{60} molecules. At low coverage, 70% of PTCDA molecules in the film form CT complexes with C_{60}. The rate of CT complex formation decreases dramatically with the beginning of the photopolymerization after 11 min of deposition. The results prove the importance of preventing the formation of $C_{60}-C_{60}$ pairs in order to keep the maximum ratio of CT complexes in the film under laser irradiation.

Introduction

Among the fullerenes, C_{60} has been the most widely studied due to its elegant molecular symmetry and intriguing structural, dynamic, and electronic properties.[1−4] Recently, there has been great interest in the development of C_{60}-based materials because they display a rich variety of solid-state properties such as superconductivity, magnetic ordering, nonlinear optical properties. It is known that C_{60} has strong electron-transfer interactions with donors.[1,4] The substantial complexation of a donor with C_{60} results not only from a strong charge transfer (CT) interaction but also from the fact that the donor molecule is able to cover closely the C_{60} molecules.[5] For this purpose, a lot of planar donors, such as tetrathiafulvalene, dithiadiazafulvalene, tetrathiotetracene, and pyranylidene families, have been widely investigated for the formation of donor−acceptor contacts with C_{60}.[6,7] These molecules are rather weak donors, with ionization potentials (IP) of 5.7−7.1 eV, and form CT complexes with C_{60} at different CT rates. In comparison with the rotationally disordered structure of C_{60}, these C_{60}-based CT complexes exhibit the lowest number of $C_{60}-C_{60}$ neighbors and a correspondingly high number of donor−acceptor contacts.[5] It was also revealed that the CT from donors to C_{60} and the deviation from the planarity in the geometry of the donors according to the formation of CT complexes affect the vibrational properties and electronic transitions.[5]

A prototype organic semiconductor 3,4,9,10-perylenetetracarboxylic dianhydride (PTCDA) has been used as a model system for the growth of organic layers by organic molecular beam deposition (OMBD) under ultrahigh vacuum (UHV) condition.[8−18] Due to its planar molecular structure and donor character (IP = 6.2 eV),[19] it can also be used as a model system for the growth of a donor−acceptor CT complex with C_{60} using OMBD. Another advantage is that PTCDA films as well as crystals have been very well characterized, so that the change upon the formation of a CT complex can easily be distinguished.

Raman and photoluminescence spectroscopies are well-known as versatile tools for the analysis of thin organic films, combining high spatial resolution, contactless and nondestructive character, the possibility of in situ thin-film characterization, and online monitoring of the growth process.[11,13,16,20,21] When characterizing the growth of a PTCDA-C_{60} complex film, the growth of the isolated PTCDA and C_{60} should also be considered. C_{60} is well-known to undergo a photopolymerization upon laser irradiation via a 2+2 cycloaddition reaction.[3,20−23] Upon photopolymerization, Raman and PL spectra change significantly. In particular, the pentagonal pinch mode $A_g(2)$ at 1468 cm^{-1} in the Raman spectra shifts toward lower frequency leading to a broad feature centered at 1459 cm^{-1}. Recently, the growth of C_{60} on different semiconductor surfaces was monitored in situ and online by combining Raman and photoluminescence (PL) spectroscopy.[20,21] This combined technique revealed that two different phases in the growth can be distinguished. At C_{60} coverages below approximately 15 nm, the photopolymerization is suppressed. Both Raman and PL spectra in this region show only features corresponding to pristine C_{60}, namely the $A_g(2)$ mode at 1468 cm^{-1} and a broad PL feature centered at 750 nm, respectively. Upon further deposition of C_{60}, photopolymerization can occur leading to a downshift of the $A_g(2)$ mode and a new feature at 820 nm in Raman and PL spectra, respectively. On the other hand, the Raman and PL spectra of PTCDA do not show any spectral change during growth.[11,13] This enables us to distinguish the formation of CT complexes with C_{60} more easily from the change in features corresponding to PTCDA.

In this paper, we will present Raman and PL spectra taken quasi-simultaneously for the growth of a PTCDA-C_{60} CT complex film under UHV condition. The formation of the PTCDA-C_{60} CT complex results in significant changes of the feature due to the C−H bending vibrational mode of PTCDA. The fraction of PTCDA molecules forming the CT complex is found to decrease according to the degree of the photopolymerization between C_{60} molecules. This result implies that it is very important to control the equivalent between donor and acceptor in order to get a higher CT complex formation rate.

* To whom correspondence should be addressed. E-mail: sunggook@physik.tu-chemnitz.de. Tel: +49-371-531-3088. Fax: +49-371-531-3060.
† Halbleiterphysik, TU Chemnitz.
‡ Institute of Semiconductor Physics.

10.1021/jp011931f CCC: $20.00
Published on Web 11/03/2001

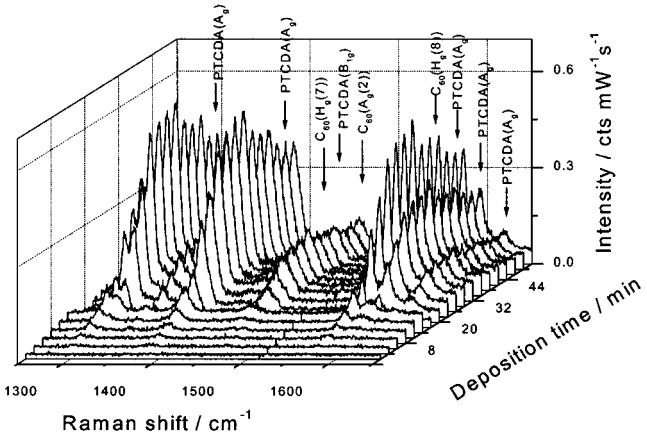

Figure 1. Raman monitoring as a function of deposition time during the co-deposition of PTCDA and C_{60} on H−Si(111)−(1 × 1).

Experimental Section

The PTCDA-C_{60} films were prepared in an UHV chamber equipped with PTCDA and C_{60} Knudsen cells. The base pressure of the chamber was 3×10^{-10} mbar. As a substrate, p-type Si(111) (R = 3 ∼ 6 Ω·cm) was used. The substrates were chemically pretreated by immerging into hydrogen fluoride (HF, 40%) solution for 2 min to remove the oxide layer from the surface and passivating the surface with hydrogen. Then, the sample was introduced into the UHV chamber. The surface shows a (1 × 1) reconstruction by low electron energy diffraction (LEED) pattern. As preliminary experiments, respective PTCDA and C_{60} were deposited onto such surfaces treated under identical conditions. The PTCDA and C_{60} Knudsen cells were operated at 280 °C and 400 °C with deposition rates of 1 nm/min and 3 nm/min, respectively. The Raman intensity for a C_{60} film is found to be much lower than that of a PTCDA film at a same thickness. Therefore, the deposition ratio PTCDA/C_{60} = $^1/_3$ was also applied during growth of co-deposited film. This also makes it easier to distinguish changes in the vibrational modes corresponding to PTCDA upon CT complex formation because all PTCDA molecules are expected to have a similar environment surrounded by a larger amount of C_{60} molecules. Because the film thickness of the co-deposited film is not exactly known, the deposition time serves as a parameter in the results.

The UHV chamber is optically aligned to a triple monochromator (Dilor XY) and a single monochromator used for Raman and photoluminescence (PL) measurements, respectively. A CCD camera was used for multichannel detection. Raman and PL spectra were taken in situ and online during the co-deposition of PTCDA and C_{60} onto the substrate. Both Raman and photoluminescence spectra were taken during a deposition series by changing the optical path for each monochromator every 90 s. This enables to avoid the experimental error that could occur between different deposition series. An Ar^+ laser (488 nm, P_{flux} = 28 W/cm^2) was used for excitation focused on the substrate to a spot of approximately 300 μm in diameter. This laser line shows the strongest resonant condition in the Raman spectra of PTCDA. All spectra were taken in a backscattering geometry. Accumulation times of 1 min and 2 s were used for Raman and photoluminescence measurements, respectively.

Results and Discussion

Figure 1 displays the evolution of Raman spectra as a function of deposition time in the spectral range of 1250−1650 cm^{-1} during co-deposition of PTCDA and C_{60} on H−Si(111)−(1 × 1) surfaces. Previous measurements and theoretical calculations have shown that the most intensive features of both PTCDA and C_{60} exist in this spectral range.[3,11−13,18,20−25] The featureless spectrum at 0 min corresponds to the hydrogen passivated Si(111) surface. As the deposition goes on, new features appear due to inelastic scattering of co-deposited PTCDA and C_{60}. The peaks are assigned according to previous Raman studies of C_{60} and PTCDA films[2,18,24] and they are presented with their symmetry in Table 1. Although a higher evaporation rate was used for C_{60}, the intensity of its most intensive feature, namely $A_g(2)$ mode of C_{60} in the region of 1450−1468 cm^{-1}, is much lower than peaks corresponding to PTCDA at 1305, 1381, and 1572 cm^{-1}. This is in good agreement with the results of the preliminary deposition of bare PTCDA and C_{60} films. In addition, a modulation of the intensity was observed during the growth, which is attributed to a Fabry−Perot interference effect of the incident and scattered light within the layer. Upon a close look at the spectra, changes can be seen in the regions of 1295−1340 cm^{-1} and 1450−1470 cm^{-1}. The former corresponds to A_g C−H bending modes of PTCDA and the latter to the pentagonal pinch $A_g(2)$ mode of C_{60}. Because a higher evaporation rate was used for C_{60}, it is expected that the probability of a C_{60} molecule neighboring to another C_{60} molecule is rather high, thus favoring photopolymerization upon laser irradiation. In the following, we will examine these spectral regions of the A_g C−H bending modes of PTCDA and the $A_g(2)$ mode of C_{60} in more detail.

Figure 2 shows the Raman spectra in the spectral region of 1250−1450 cm^{-1} as a function of deposition time. In this region, only two strong A_g C−H bending modes of PTCDA at 1305 and 1381 cm^{-1} exist, whereas there is only a weak feature at 1426 cm^{-1} corresponding to C_{60}. Therefore, the changes in the vibrational modes of PTCDA due to the co-deposition of C_{60} and PTCDA can easily be detected in this region. From the

TABLE 1: Frequency Positions Observed in Raman Spectra of PTCDA, C_{60}, and PTCDA-C_{60} Complex Films with Their Symmetry[a]

PTCDA			C_{60}			PTCDA-C_{60}	
wavenumber/cm^{-1}		symmetry	wavenumber/cm^{-1}		symmetry	wavenumber/cm^{-1}	
233	w	A_g C−O				233	w
			268	w	H_g	268	w
431	w	B_{1g}	431	vw		431	vw
			493	vw	$A_g(1)$		
538	w	A_g ring deform.				538	w
624	w	A_g ring deform.				624	w
			707	w	H_g		
725	vw	A_g ring deform.					
			773	vw	H_g		
1051	w	A_g C−H bend.				1051	w
			1242	vw	H_g		
						1295	vs
1305	vs	A_g C−H bend.				1305	vs
						1338	w
1381	s	A_g C−H bend.				1381	vs
			1426	m	H_g		
						1431	w
1451	w	B_{1g} ring str.				1451	m
						1455	m
			1459	s	$A_g(2)$	1459	m
			1567	m	H_g		
1572	s	A_g C−C str.				1573	s
1591	s	A_g C−C str.				1592	s
1617	w	A_g C−H str.				1617	w

[a] The symmetry is referenced from previous studies of Eklund et al.[2], Scholz et al.,[18] and Akers et al.[24] Bold numbers represent features appearing only for the PTCDA-C_{60} complex films. s = strong, m = medium, w = weak, v = very.

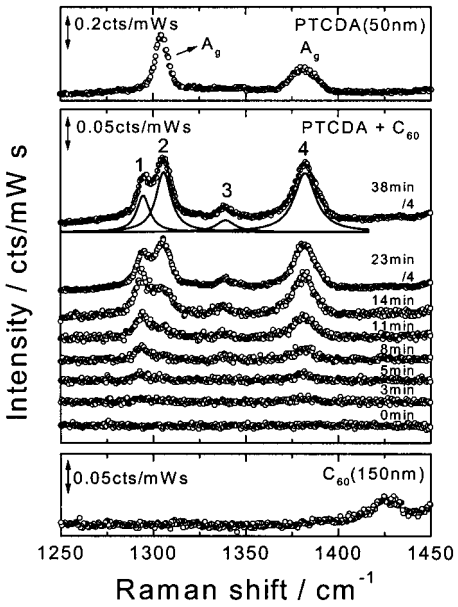

Figure 2. Individual Raman spectra in the spectral range of 1250−1450 cm^{-1} during the co-deposition of PTCDA and C_{60} on H−Si(111)−(1 × 1). A representative 4-Lorentzian curve fitting result is included at the spectrum of 38 min. For comparison, the Raman spectra for 50 nm PTCDA (upper spectrum) and 150 nm C_{60} (lower spectrum) films are included.

beginning of the deposition features at 1295 and 1381 cm^{-1} denoted peaks 1 and 4 in Figure 2 appear. At the shoulder on the right-hand side of the 1295 cm^{-1} feature, an additional small feature is seen at 1305 cm^{-1} (peak 2). This small feature corresponds to an A_g C−H bending mode of PTCDA, whereas the feature at 1295 cm^{-1} is new and should be related to the formation of PTCDA-C_{60} CT complexes. As the thickness of the film increases, the intensity of the peak at 1305 cm^{-1} with respect to that at 1295 cm^{-1} increases. This indicates an increasing portion of PTCDA molecules that do not form CT complexes with C_{60}. The spectra taken after 23 min are all identical in line shape. An additional new feature has also appeared at 1338 cm^{-1} (peak 3) and increases with increasing deposition time. According to a Raman study of PTCDA films by Akers et al.,[24] strong peaks at 1294 and 1341 cm^{-1} were observed when a nonresonance laser line at 647.1 nm was used or when a surface-enhanced Raman (SER) spectrum was taken from PTCDA on silver (Ag) islands using resonant laser lines at 488 and 514.5 nm. However, these features were suppressed without SER conditions even though 488 and 514.5 nm lines were used. They were interpreted as being a result of a lifting of the selection rules.[24] Most probably, the charge transfer between Ag and PTCDA in the SERS condition leads to the excitation of the vibrational mode that is forbidden in a non-SER condition. The appearance of the peaks at 1295 and 1338 cm^{-1} in the PTCDA and C_{60} coevaporated film indicates the formation of the charge transfer between two molecules, violating the selection rules of bare PTCDA films. Thus, it can be concluded that there are two different chemical states of PTCDA molecules existing in the coevaporated film, one of bare PTCDA and the other corresponding to PTCDA forming CT complexes with C_{60}. Moreover, the ratio of the peak intensities at 1295 cm^{-1} with respect to that of 1305 cm^{-1} is indicative of the amount of the PTCDA forming CT complexes with C_{60}.

To quantitatively understand structural changes during the co-deposition of C_{60} and PTCDA, the four peaks at 1295, 1305, 1338, and 1381 cm^{-1} were curve fitted using four Lorentzian functions. A representative curve fitting result is presented in the topmost spectra for co-deposited film in Figure 2. These four peaks are labeled 1−4. For peak 3, curve fitting was difficult below a deposition time of 5 min due to its low intensity. For all peaks, no shift in the frequency positions is observed during the deposition. The full widths at half maximum (FWHMs) are also constant except for that of peak 3, which is shown in Figure 3. The FWHM increases continuously and reaches 13 cm^{-1} after 23 min, i.e., the same time at which the intensity ratio of peaks 1 to 2 reaches a constant value (Figure 2). A close look at the spectra in the region of peak 3 (inset in Figure 3) reveals the presence of a small shoulder at the high frequency side after 23 min, which does not exist or is too weak to be observed at 14 min. The increase of this shoulder seems to contribute to the increase in the FWHM of peak 3. The FWHMs for peaks 2 and 4 agree well with the previously reported values of 9.8 and 13.7 cm^{-1} for a PTCDA film.[18]

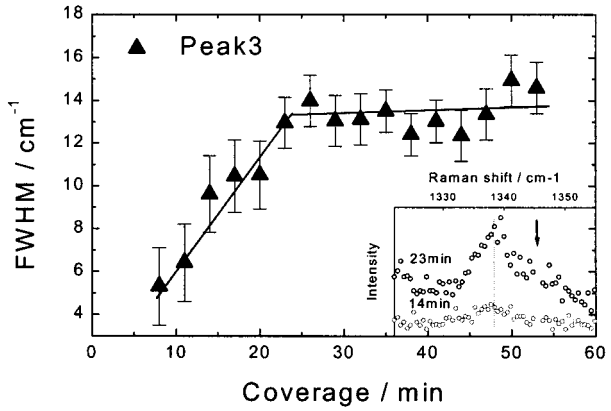

Figure 3. Time evolution of the FWHM corresponding to peak 3 at 1338 cm^{-1} during the co-deposition of PTCDA and C_{60} on H−Si(111)−(1 × 1). A solid line is included as a guide for the eyes. The spectra in the region of peak 3 at 14 and 23 min of deposition are represented in the inset.

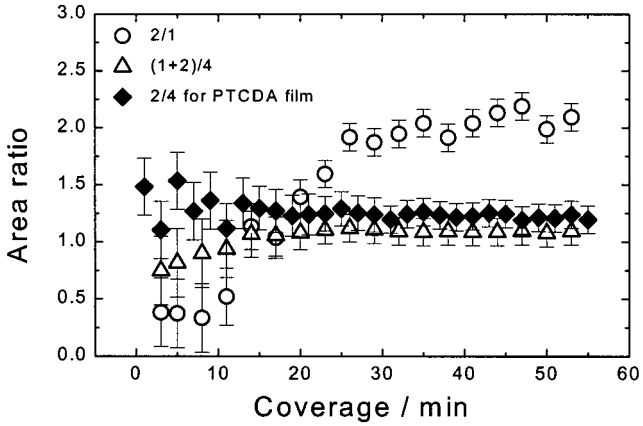

Figure 4. Time evolution of the area ratio between two peaks. ○ and △ represent area ratio between peaks 1 and 2, and the sum of area for peaks 1 and 2 divided by the area of peak 4 for the PTCDA-C_{60} co-deposited film. ◆ represents area ratio between peaks 2 and 4 for bare PTCDA film.

The relative area between peaks 1 and 2 clearly illustrates the change in the amount of PTCDA molecules forming PTCDA-C_{60} CT complexes during growth (circles in Figure 4). Below a deposition time of 8 min, the relative area between peaks 1 and 2 is constant. As the deposition continues, the area for peak 2 increases strongly with respect to peak 1 indicating an increasing portion of PTCDA that does not form PTCDA-C_{60} complexes. After 23 min, the area ratio remains constant again.

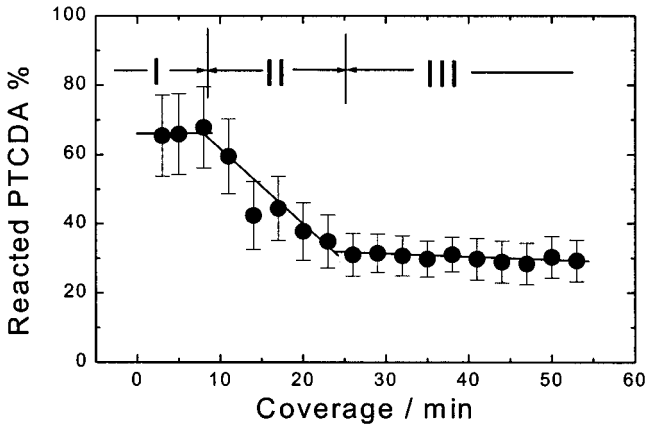

Figure 5. The fraction of PTCDA in the co-deposited film forming CT complexes with C_{60}. A solid line is included as a guide for the eyes.

Despite the change in relative area, however, the sum of the areas for peaks 1 and 2 is almost constant during the entire deposition time when normalized to peak 4 (triangles in Figure 4). Additionally, this sum of the areas for peaks 1 and 2 with respect to peak 4 agrees well with the area ratio of peak 2/peak 4 for a bare PTCDA film (diamonds in Figure 4). Assuming that the sum of the area for peaks 1 and 2 is indicative of the total number of PTCDA in the film, a fraction of PTCDA molecules forming CT complexes with C_{60} can be estimated (see Figure 5). The behavior observed can be divided into three regimes. In the first regime, 70% of PTCDA deposited form PTCDA-C_{60} complexes. In the second regime, the portion of the PTCDA forming CT complexes with C_{60} decreases. Finally, after 23 min when a constant fraction of C_{60} participates in the photopolymerisation, only 30% of PTCDA in the film takes part in the PTCDA-C_{60} complex formation.

The reason the chemical composition of the PTCDA-C_{60} CT complex film changes during the deposition can be found by looking at the spectra in the region of the $A_g(2)$ mode of C_{60}. Raman spectra in this range of 1420−1500 cm^{-1} are presented in Figure 6 as a function of deposition time. For comparison, the spectra taken for thick films of C_{60} (150 nm) and PTCDA (50 nm) are again included. In this spectral region, the $H_g(7)$ and $A_g(2)$ modes of C_{60} exist centered at 1426 and 1459 cm^{-1}, respectively, and a B_{1g} ring stretch mode of PTCDA at 1451 cm^{-1}. For the spectra of the PTCDA-C_{60} co-deposited film, it should be first mentioned that the signal-to-noise ratio is fairly weak. Therefore, the spectra below 5 min hardly reveal any signal. After 8 min deposition, weak features centered at 1468 and 1455 cm^{-1} appear. The peak at 1468 cm^{-1} corresponds to pristine C_{60} which is expected to exist in the film due to the higher evaporation rate of C_{60} relative to that of PTCDA. From the previous Raman study for the growth of C_{60} on different substrates, it is known that photopolymerization between C_{60} molecules is suppressed at coverages below 15 nm irrespective of the substrate despite the continuous irradiation of the laser line for the Raman measurement.[20,21] It can be seen from the initial appearance of the peak at 1468 cm^{-1} corresponding to pristine C_{60} that this suppression effect also seems to hold for the co-deposited film. On the other hand, the new feature at 1455 cm^{-1} indicates the formation of C_{60}−PTCDA complexes. According to Dresselhaus et al.,[22] Raman spectra of solid C_{60} doped with different alkali metals show a softening of the $A_g(2)$ mode at 1468 cm^{-1}, resulting in downshift of the peak. The more CT occurs, the more the position of $A_g(2)$ mode shifts toward lower frequency. Therefore, the softening of $A_g(2)$ mode is an indication of CT to C_{60}. This behavior was also observed

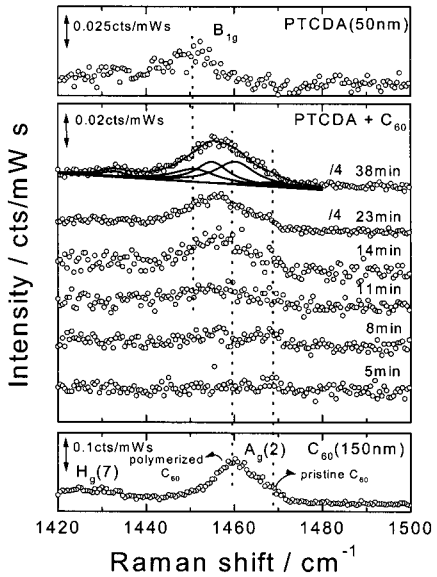

Figure 6. Individual Raman spectra in the vicinity of the pentagonal pinch mode $A_g(2)$ of C_{60} during the co-deposition of PTCDA and C_{60} on H−Si(111)−(1 × 1). For comparison, the Raman spectra for thick PTCDA (upper spectrum) and C_{60} (lower spectrum) are included. Dot lines included indicate the frequency positions corresponding to B_{1g} mode of bare PTCDA and $A_g(2)$ mode of pristine and polymerized C_{60}.

for a molecular CT complex TDAE-C_{60} (where TDAE is tetrakis(dimethylamino)ethylene).[26] Upon further deposition, the broad feature centered at 1455 cm^{-1} increases relative to that at 1468 cm^{-1}. However, the curve fitting of this broad feature reveals four different components with reasonable FWHMs ranging 6.5−12 cm^{-1}. From the fitting, the peak at 1459 cm^{-1} increases between 11 and 23 min with respect to that at 1468 cm^{-1}, which indicates the photopolymerization of C_{60}. Besides, a lower frequency shoulder of the peak at 1455 cm^{-1} can be recognized, which can be attributed to a B_{1g} ring stretch mode of PTCDA. After 23 min, no more changes occur in the spectra. The time is again in agreement with the time when the portion of the PTCDA molecules undergoing the formation of CT complexes with C_{60} and the FWHM of the peak at 1338 cm^{-1} becomes constant.

The photopolymerization between C_{60} molecules is a time-dependent process depending on the laser power used. For PTCDA-C_{60} CT complexes there should be no slow measurable rate of formation and they should be instantaneously formed as the two species are co-deposited in a uniform manner. Thus, these two processes should occur in sequence. Because the higher evaporation rate is used for C_{60}, most of the PTCDA molecules deposited are expected to form CT complexes with C_{60} instantaneously, followed by the breakage of the complexes as the photopolymerization between C_{60} molecules proceeds. However, the Raman spectrum measured post-growth with longer accumulation time (10 min) shows an identical line shape of the pentagonal pinch mode region of C_{60} to that during the growth (accumulation time = 1min), except for the deposition time when the photopolymerization is suppressed. The only difference is the signal-to-noise ratio. This indicates that the photopolymerization at this laser power completes within the accumulation time (1 min) for the Raman measurement and, thus, the spectral change cannot be influenced by the time-dependent transient of photopolymerization. Therefore, the measured spectra can be considered to be those in quasi-equilibrium states at each deposition time and they may be different if a different laser power is used.

Upon photopolymerization between C_{60} molecules various polymeric states can be formed, depending on the laser power and the substrate temperature used for the growth.[20,21,27] The density functional tight binding (DF-TB) energy difference between the different oligomers and isolated C_{60} molecules calculated by Porezag et al.[27,28] shows that the formation of dimers is most probable and that the formation of higher oligomers needs higher energy. They also calculated the Raman frequencies and intensities for different oligomeric C_{60}. According to their calculation, the broad peak centered at 1459 cm^{-1} in the preliminary Raman results of the C_{60} growth (lowest spectrum in Figure 6) indicates that the film with the laser power used consists mainly of dimers. Thus, even though the formation energy of a PTCDA-C_{60}- CT complex is not known, it is unlikely that CT complexes of a dimeric C_{60} with PTCDA (PTCDA $-C_{60}-C_{60}$) can form. Accordingly, the polymeric state of C_{60} in the CT complex film is expected to be dimers.

Altogether, there are two processes occurring during the co-deposition of PTCDA and C_{60}, namely the formation of CT complexes between two species and the photopolymerization between C_{60} molecules. The PTCDA-C_{60} CT complexes are formed instantaneously upon co-deposition. The breakage of the CT complexes follows according to the degree of the photopolymerization of C_{60} and C_{60} dimers are mainly formed. Therefore, in the regime where the photopolymerization between C_{60} is suppressed, a higher rate of $C_{60}-$PTCDA CT complexes formed upon co-deposition remains, whereas this rate decreases with the beginning of the photopolymerization of C_{60}. After 23 min, no more changes occur, indicating the constant ratio between the formation of the CT complexes and the photopolymerization of C_{60}. Since the photopolymerization can break the CT complexes only when an excess C_{60} is neighboring to a CT complex, this result suggests that in designing an acceptor−donor complex with C_{60} it is very important to reduce the number of $C_{60}-C_{60}$ pairs in the film in order to keep the maximum number of CT complexes under the laser illumination.

After growth the Raman spectrum was measured in the region of 50−1700 cm^{-1} and the positions of features observed are presented in Table 1. The frequency positions in the table were taken at maximum peak positions in the spectra without further fitting procedure. There are four features at 1295, 1338, 1431, and 1455 cm^{-1} observed only for the PTCDA-C_{60} complex film. Except these four peaks and even though some weak features of bare C_{60} and PTCDA were not observed for the PTCDA-C_{60} complex film, the spectrum seems to be merely a superposition of spectra corresponding to bare C_{60} and PTCDA films.

The PL spectra during the co-deposition of C_{60} and PTCDA as a function of deposition time are presented in Figure 7. Each spectrum was accumulated for 2 s. The spectra can again be compared to those for thick C_{60} and PTCDA films. The PL spectrum for the PTCDA film was measured at −192 °C, whereas that for C_{60} at RT. The lowest spectrum (0 min) corresponds to the H−Si(111)−(1 × 1) surface. During the co-deposition of C_{60} and PTCDA significant changes can be observed in the spectra. At low coverage, i.e., at a deposition time of 4 min, a feature appears at 700 nm (peak C). In this region, the film consists of 70% of PTCDA forming PTCDA-C_{60} CT complex, 30% of PTCDA, and excess pristine C_{60}, as judged from Raman spectra. However, the features corresponding to PTCDA and pristine C_{60} are hardly seen. The feature at around 700 nm was observed for C_{60} crystals grown from purified powder[29] and highly pressurized C_{60}.[23,30] It was interpreted as resulting from transitions of C_{60} molecules located in an imperfect crystal environment, such as molecules adjacent to chemical impurities, to crystal defects, or to crystal surface,[29−31] resulting in emissions from transitions which are forbidden in isolated C_{60}. Such imperfection can possibly occur during the PTCDA-C_{60} CT formation, resulting in the feature at 700 nm. For the spectra at 10 and 13 min at which the rate of the complexation between C_{60} and PTCDA begins to decrease, a PL peak centered at 750 nm appears (peak A). By comparison of PL spectra for bare C_{60} and PTCDA films, the feature centered at 750 nm seems to be mostly due to emission from C_{60}. With increasing deposition time, the peak A at 750 nm shifts toward lower wavelength and a new feature at 660 nm (peak B) can be observed. Both indicate the increasing contribution of emissions from PTCDA molecules, which is in a good agreement with the Raman results. No more change in PL spectra is observed after a deposition time of 23 min, which also agrees well with the results from the Raman spectra.

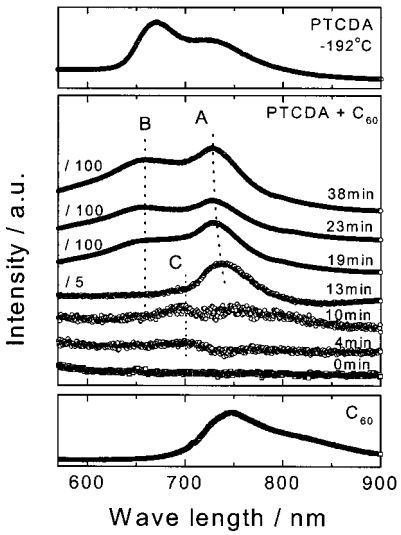

Figure 7. Photoluminescence spectra during the co-deposition of PTCDA and C_{60} on H−Si(111)−(1 × 1). For comparison, the PL spectra for 50 nm PTCDA (upper spectrum) and 150 nm C_{60} (lower spectrum) are included.

Summary

In situ and online Raman and PL spectroscopies were employed during the growth of a PTCDA-C_{60} CT complex film on hydrogen passivated Si(111)−(1 × 1) using OMBD. Significant changes in the C−H bending vibrational modes of PTCDA and Ag(2) mode of C_{60} indicate the formation of CT complexes. From the intensity ratio between the Raman peaks at 1305 cm^{-1} corresponding to pristine PTCDA and at 1295 cm^{-1} originated from PTCDA-C_{60} CT complexes, the ratio of PTCDA molecules involved in the CT formation was estimated. Upon co-deposition of the two species, 70% of PTCDA molecules in the film are found to take part in the CT formation with C_{60}. It reduces with the beginning of the photopolymerization between C_{60} molecules and after 23 min it reaches 30%. The change in Raman spectra agrees very well with that in PL spectra. The results indicate that in order to keep the maximum number of CT complexes in the film under laser irradiation, the neighboring of C_{60} to other C_{60} should be kept at the minimum possible. It is also proven that PTCDA, which has been widely investigated as a model system for OMBD, can be also used as a donor for the formation of a donor−acceptor complex using OMBD.

Acknowledgment. We thank the Bundesministerium für Bildung und Forschung (BMBF) for the financial support under Grant No. 05 SE8OCA 7. Additional support by the EU funded Human Potential Research Training Network "DIODE" (Contract No. HPRN-CT-1999-00164) is gratefully acknowledged.

References and Notes

(1) Graja, A. *Fullerene Sci. Tech.* **1997**, *5* (6), 1219.
(2) Eklund, P. C.; Rao, A. M.; Zhou, P.; Wang, Y.; J. Holden, M. *Thin Solid Films* **1995**, *257*, 185.
(3) Dresselhaus, M. S.; Dresselhaus, G.; Eklund, P. C. *Science of Fullerences and Carbon Nanotubes*; Academic: New York, 1996.
(4) Ouyang, M.; Xue, Z. Q.; Wang, K. Z.; Wu, Q. D.; Qiang, D. *J. Vac. Sci. Technol. B* **1997**, *15* (4), 1304.
(5) Graja, A.; Farges, J. *Adv. Mater. Opt. Electron.* **1998**, *8*, 215.
(6) Spitsina, N. G.; Semkin, V. N.; Lapinski, A.; Krol, S.; Graja, A. *Fullerene Sci. Technol.* **1995**, *3*, 511.
(7) Spitsina, N. G.; Semkin, V. N.; Graja, A. *Acta Phys. Polon. A* **1995**, *87*, 869.
(8) Forrest, S. R. *Chem. Rev.* **1997**, *91*, 1793.
(9) Glöckler, K.; Seidel, C.; Soukopp, A.; Sokolowski, M.; Umbach, E.; Böhringer, M.; Berndt, R.; Schneider, W.-D. *Surf. Sci.* **1998**, *405*, 1.
(10) Umbach, E.; Sokolowski, M.; Fink, R. *Appl. Phys. A* **1996**, *63*, 565.
(11) Kampen, T. U.; Tenne, D. A.; Park, S.; Salvan, G.; Scholz, R.; Zahn, D. R. T. *Phys. Stat. Sol. B* **1999**, *215*, 431.
(12) Kampen, T. U.; Rossow, U.; Schumann, M.; Park, S.; Zahn, D. R. T. *J. Vac. Sci. Technol. B* **2000**, *18* (4), 2077.
(13) Kampen, T. U.; Salvan, G.; Friedrich, M.; Tenne, D. A.; Park, S.; Zahn, D. R. T. *Appl. Surf. Sci.* **2000**, *166*, 387.
(14) Park, S.; Querner, T.; Kampen, T. U.; Braun, W.; Zahn, D. R. T. *Appl. Surf. Sci.* **2000**, *166*, 376.
(15) Park, S.; Kampen, T. U.; Zahn, D. R. T.; Braun, W. *Appl. Phys. Lett.* **2000**, *76*, *22*, 3200.
(16) Tenne, D. A.; Park, S.; Kampen, T. U.; Das, A.; Scholtz, R.; Zahn, D. R. T. *Phys. Rev. B* **2000**, *61* (21), 14 564.
(17) Ogawa, T.; Kuwamoto, K.; Isada, S.; Kobayashi, T.; Karl, N. *Acta Crystallogr. B* **1999**, *55*, 123.
(18) Scholz, R.; Kobitski, A. Yu.; Kampen, T. U.; Schreiber, M.; Zahn, D. R. T.; Jungnickel, G.; Elstner, M.; Sternberg, M.; Frauenheim, Th. *Phys. Rev. B* **2000**, *61* (20), 13 659.
(19) Ishii, H.; Sugiyama, K.; Ito, E.; Seki, K. *Adv. Mater.* **1999**, *11* (8), 605.
(20) Park, S.; Han, H.; Kaiser, R.; Werninghaus, T.; Schneider, A.; Drews, D.; Zahn, D. R. T. *J. Appl. Phys.* **1998**, *84* (3), 1340.
(21) Drews, D.; Zahn, D. R. T. *Carbon* **1998**, *36* (5−6), 645.
(22) Dresselhaus, M. S.; Dresselhaus, G.; Eklund, P. C. *J. Raman Spectrosc.* **1996**, *27*, 351.
(23) Rao, A. M.; Eklund, P. C.; Venkateswaran, U. D.; Tucker, J.; Duncan, M. A.; Bendele, G. M.; Stephens, P. W.; Hodeau, J.-L.; Marques, L.; Nunez-Regueiro, M.; Bashkin, I. O.; Ponyatovsky, E. G.; Morovsky, A. P. *Appl. Phys. A* **1997**, *64*, 231.
(24) Akers, K.; Aroca, R. *J. Phys. Chem.* **1987**, *91*, 2954.
(25) Salvan, G.; Tenne, D. A.; Das, A.; Kampen, T. U.; Zahn, D. R. T. *Org. Electron.* **2000**, *1*, 49.
(26) Pokhodnia, K.; Demsar, J.; Omerzu, A.; Mihailovic, D.; Kuzmany, H. *Phys. Rev. B* **1997**, *55* (6), 3757.
(27) Porezag, D. Ph.D. Thesis, Technical University of Chemnitz, 1997.
(28) Porezag, D.; Jungnickel, G.; Frauenheim, Th.; Seifert, G.; Ayuela, A.; Pederson, M. R. *Appl. Phys. A* **1997**, *64*, 321.
(29) Venkateswaran, U. D.; Schall, M. G.; Wang, Y.; Zhou, P.; Eklund, P. C. *Solid State Commun.* **1995**, *96*, 951.
(30) Kozlov, M. E.; Tokumoto, M.; Yakushi, K. *Appl. Phys. A* **1997**, *64*, 241.
(31) Guss, W.; Feldman, J.; Göbel, E. O.; Taliani, C.; Mohn, H.; Müller, W.; Häussler, P.; ter Meer, H.-U. *Phys. Rev. Lett.* **1994**, *72*, 2644.